

## Supplementary Materials

# High-content single-cell analysis on-chip using a laser microarray scanner

Jing Zhou<sup>1,2,†</sup>, Yu Wu<sup>2,†</sup>, Sang-kwon Lee<sup>2,3</sup>, and Rong Fan<sup>2,4,\*</sup>

<sup>1</sup>Department of Anesthesiology, Yale School of Medicine, New Haven, CT 06520, USA; <sup>2</sup>Department of Biomedical Engineering, Yale University, New Haven, CT 06511, USA; <sup>3</sup>Department of Semiconductor Science and Technology, Chonbuk National University, Jeonju, 561-765, Korea; <sup>4</sup>Yale Comprehensive Cancer Center, New Haven, CT 06520, USA

† These authors contribute equally to this work.

\*Correspondence should be addressed to Prof. Rong Fan (E-mail: rong.fan@yale.edu, Tel: 01-203-432-9905).

**Supplementary materials include:**

**Supplementary Figures S1-S5**

**Supplementary Table S1**

## Supplementary Figures

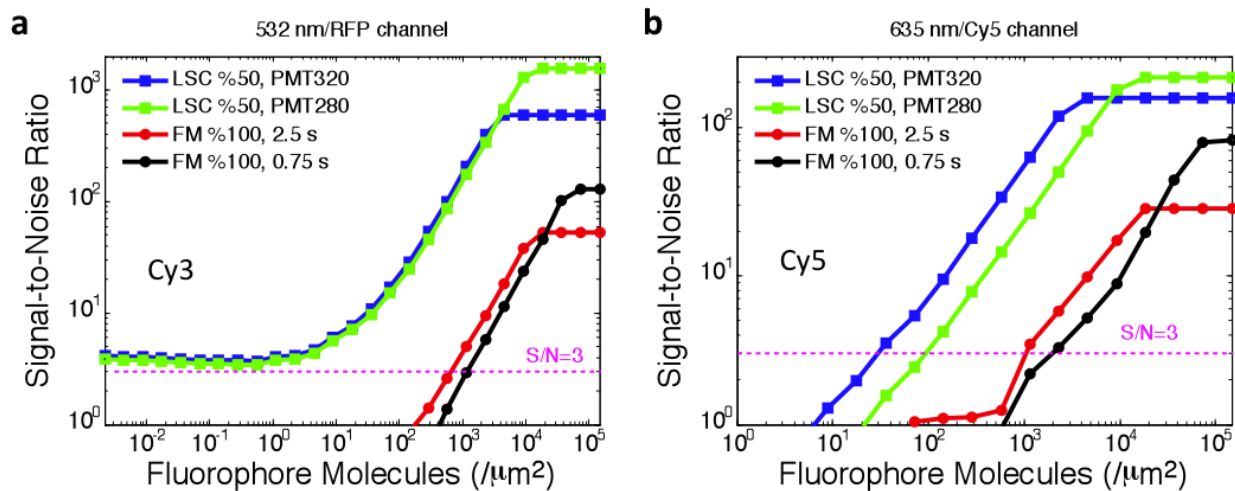


**Figure S1.** Calculation of fluorescence Signal-to-Noise Ratio (S/N) versus the surface density of fluorophores (Cy3 and Cy5). The data are derived from the original standard curves shown in Figure 2 (main text). The instrument settings are shown in the insets.

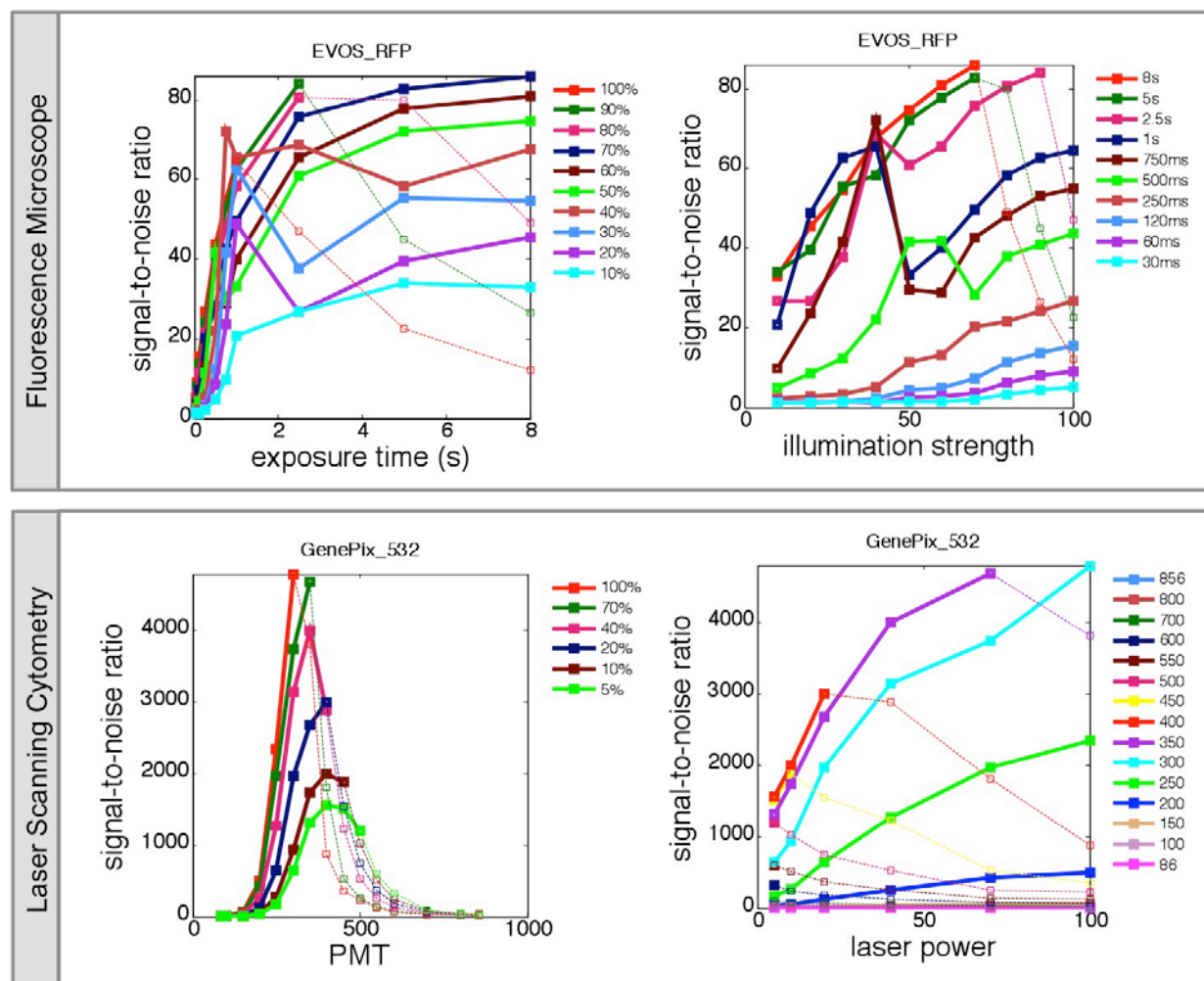


**Figure S2.** Systematic examination of the full parameter space to identify optimum imaging conditions for the green channel (Cy3 or RFP). The parameters for FM are illumination intensity and exposure time. The parameters for LSC are laser power and photomultiplier tube (PMT) gain.

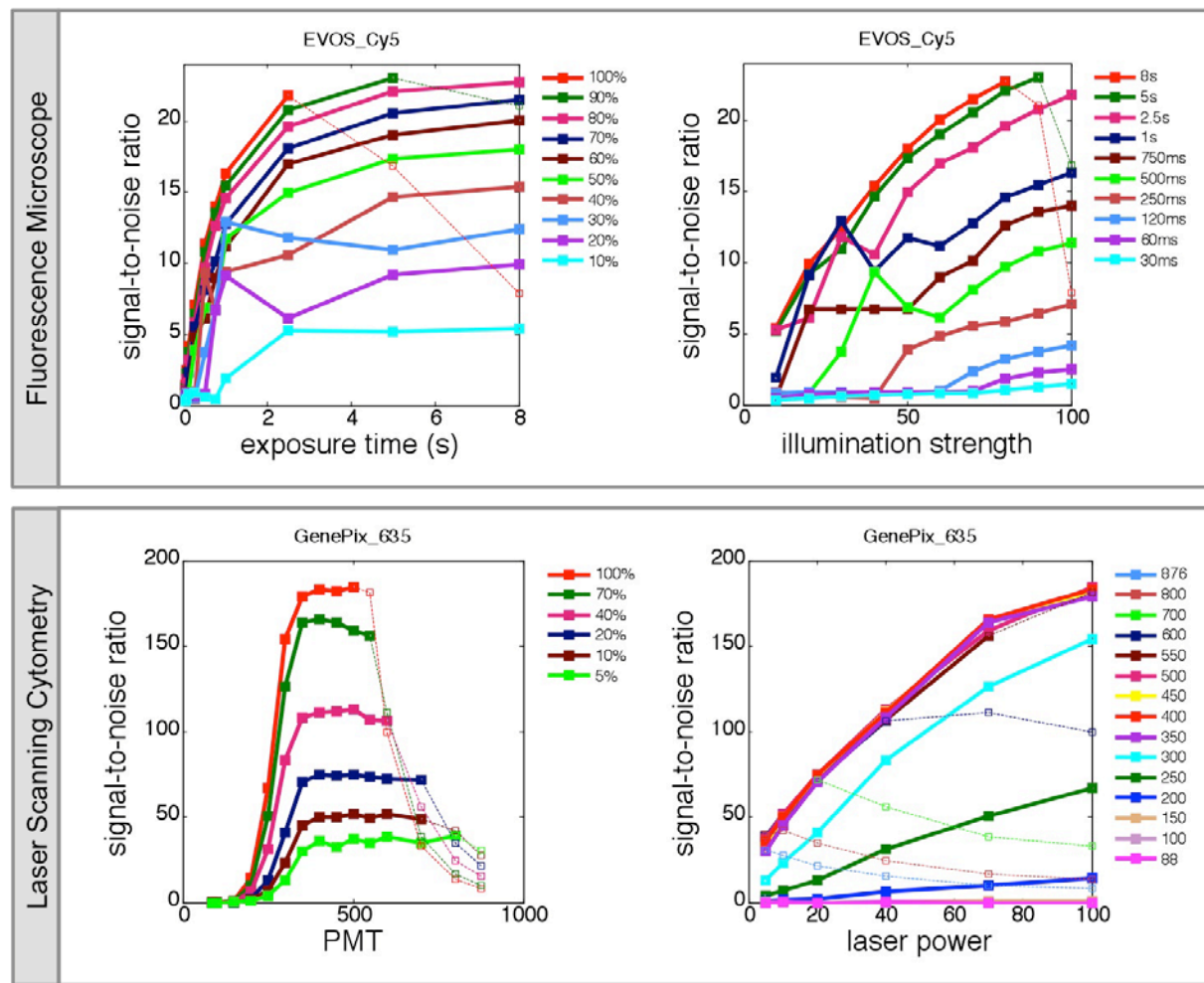


**Figure S3.** Systematic examination of the full parameter space to identify optimum imaging conditions for the red channel (Cy5). The parameters for FM are illumination intensity and exposure time. The parameters for LSC are laser power and photomultiplier tube (PMT) gain.

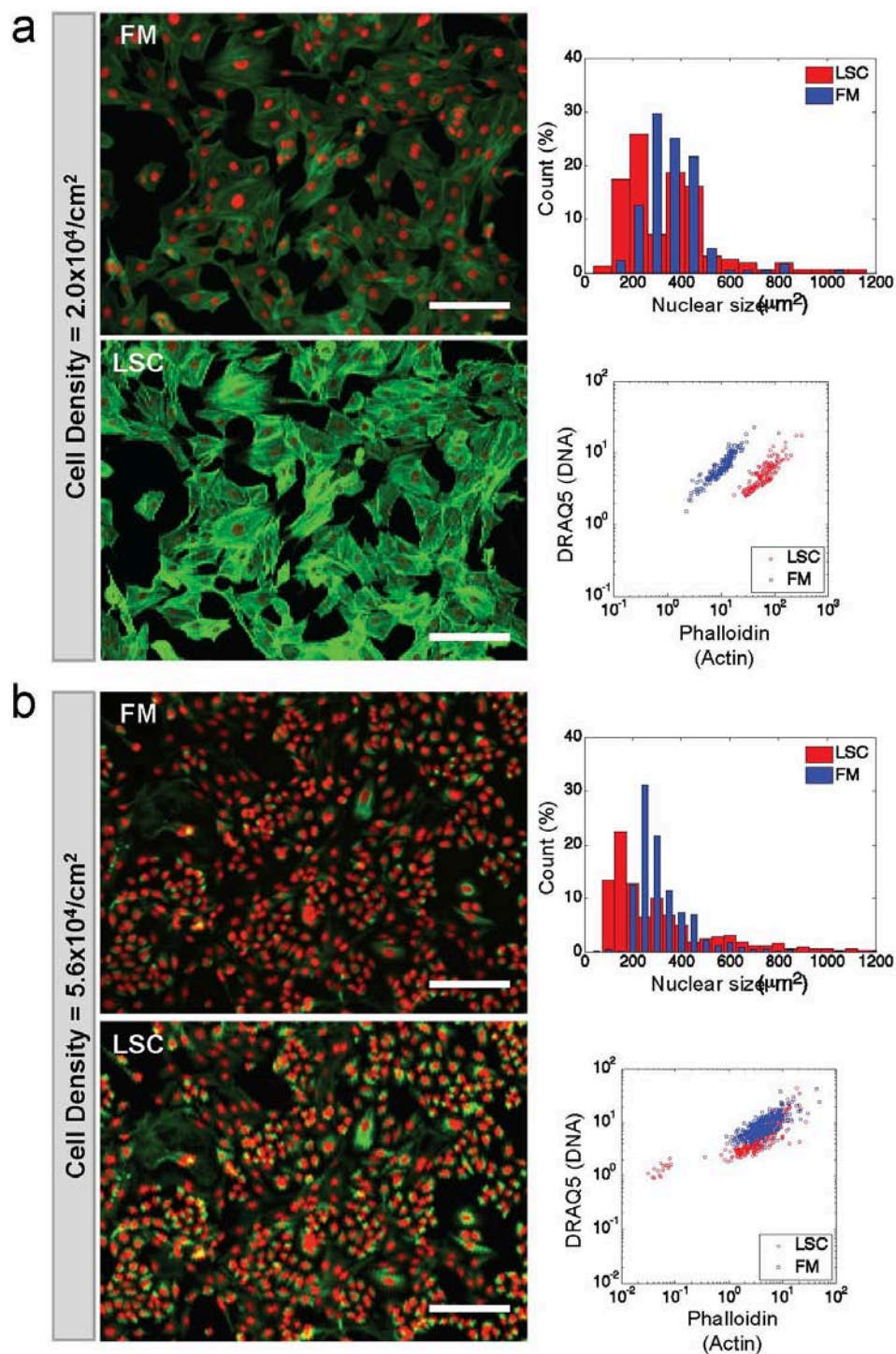


**Figure S4.** Comparison of microarray scanner-based laser scanning cytometry with conventional fluorescence microscopy for quantification of nuclear size and nuclear fluorescence signals. (a) and (b) show immunofluorescence imaging and quantitative analysis of nuclear size and genomic DNA content of the NIH/3T3 cells cultured at different cell densities. Left panels are fluorescence imaging of the same region by FM and LSC. Right panels show the histograms of nuclear size and the scatter graph (DNA vs. actin). Although FM and LSC have different dynamic range and absolute intensities that can not be directly compared, but the scatter plots are very similar in terms of distribution and the features. Scale bar:  $200\mu\text{m}$ .

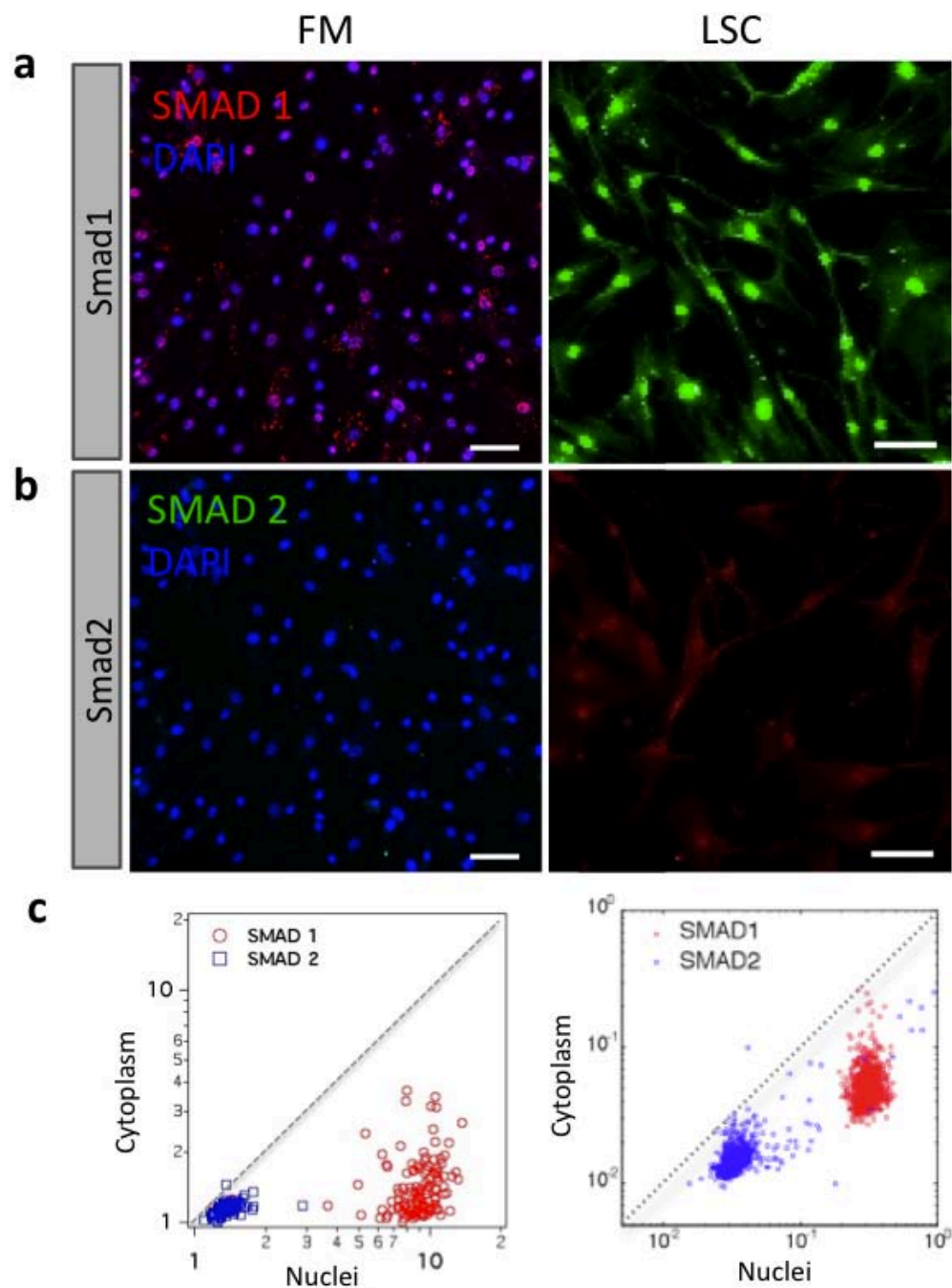


**Figure S5.** Comparison of microarray scanner-based laser scanning cytometry with conventional fluorescence microscopy for detecting nuclear localization of SMAD1 and SMAD2 in human mesenchymal cells. (a, b) Images showing immunofluorescence detection of Smad1 (a) and Smad (2) using a conventional epifluorescence microscope (FM: EVOS fl) and the laser microarray scanner (LSC). DAPI was used in the FM imaging to visualize nuclei. Apparently, Smad1 is co-localized with DAPI indicating nuclear accumulation. Scale bar: 100 $\mu$ m. (c) Scatter graphs showing quantitative analysis of Smad1 and Smad2 distribution in nucleus vs cytoplasm. Because laser microarray scanner has a larger dynamic range and better detection sensitivity, there is at least an order of magnitude detection range below the observed Smad1 and Smad2, whereas the low end of the signals in fluorescence microscope is approaching the background.

## Supplementary Table

Table S1. List of the morphometric parameters quantified in Figure 5e. More details can be found at Refs. 47 and 48

#	Parameters	Description
1	AreaShape_Area	The actual number of pixels in the region
2	AreaShape_Solidity	The proportion of the pixels in the convex hull that are also in the region. Also known as convexity. Computed as Area/Convex Area.
3	AreaShape_Zernike_0_0	Coefficients of Zernike polynomials from order 0 to order 9 are calculated, giving in total 30 measurements of Zernike shape features: measure shape by describing a binary object (or more precisely, a patch with background and an object in the center) in a basis of Zernike polynomials, using the coefficients as features.
4	AreaShape_Zernike_1_1	coefficients of order 1 Zernike polynomials
5	AreaShape_Zernike_2_0	coefficients of order 2 Zernike polynomials
6	AreaShape_Zernike_2_2	
7	AreaShape_Zernike_3_1	coefficients of order 3 Zernike polynomials
8	AreaShape_Zernike_3_3	
9	AreaShape_Zernike_4_0	coefficients of order 4 Zernike polynomials
10	AreaShape_Zernike_4_2	
11	AreaShape_Zernike_4_4	
12	AreaShape_Zernike_5_1	coefficients of order 5 Zernike polynomials
13	AreaShape_Zernike_5_3	
14	AreaShape_Zernike_5_5	
15	AreaShape_Zernike_6_0	coefficients of order 6 Zernike polynomials
16	AreaShape_Zernike_6_2	
17	AreaShape_Zernike_6_4	
18	AreaShape_Zernike_6_6	
19	AreaShape_Zernike_7_1	coefficients of order 7 Zernike polynomials
20	AreaShape_Zernike_7_3	
21	AreaShape_Zernike_7_5	
22	AreaShape_Zernike_7_7	
23	AreaShape_Zernike_8_0	coefficients of order 8 Zernike polynomials
24	AreaShape_Zernike_8_2	
25	AreaShape_Zernike_8_4	
26	AreaShape_Zernike_8_6	
27	AreaShape_Zernike_8_8	
28	AreaShape_Zernike_9_1	coefficients of order 9 Zernike polynomials
29	AreaShape_Zernike_9_3	
30	AreaShape_Zernike_9_5	
31	AreaShape_Zernike_9_7	
32	AreaShape_Zernike_9_9	